JOC The Journal of Organic Chemistry

Note

Probing Through-Space Polar–# Interactions in 2,6-Diarylphenols

Vera Bosmans, Jordi Poater, Roel Hammink, Paul Tinnemans, F. Matthias Bickelhaupt, and Jasmin Mecinovic

J. Org. Chem., **Just Accepted Manuscript** • DOI: 10.1021/acs.joc.8b03147 • Publication Date (Web): 22 Feb 2019

ACS Publications

is published by the American Chemical Society. 1155 Sixteenth Street N.W., Washington, DC 20036

Probing Through-Space Polar–π Interactions in 2,6-Diarylphenols

Vera Bosmans,[†⊥] Jordi Poater,[‡§⊥] Roel Hammink,[¶⊥] Paul Tinnemans,[†] F. Matthias Bickelhaupt,*[†∥] and Jasmin Mecinović*[†$]

[†] Institute for Molecules and Materials, Radboud University, Heyendaalseweg 135, 6525 AJ Nijmegen, The Netherlands

[‡] ICREA, Passeig Lluís Companys 23, 08010 Barcelona, Spain

[§] Departament de Química Inorgànica i Orgànica & IQTCUB, Universitat de Barcelona, Martí i Franquès 1-11, 08028 Barcelona, Spain

[¶] Department of Tumor Immunology, Radboud Institute for Molecular Life Sciences, Radboud University Medical Center, Geert Grooteplein 26, 6525 GA Nijmegen, The Netherlands

[∥] Department of Theoretical Chemistry, Amsterdam Center for Multiscale Modeling, Vrije Universiteit Amsterdam, De Boelelaan 1083, 1081 HV Amsterdam, The Netherlands

[$] Department of Physics, Chemistry and Pharmacy, University of Southern Denmark, Campusvej 55, 5230 Odense, Denmark

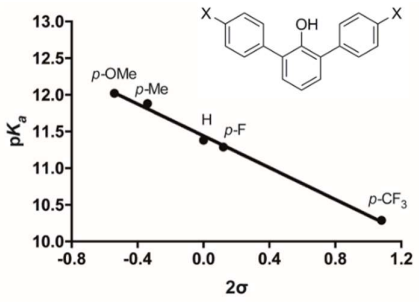

ABSTRACT: Although it is well established that the acidity of phenol can be fine-tuned with substituents on its aromatic ring *via* through-bond effects, the role of through-space effects on the acidity of phenols is presently poorly understood. Here, we present integrated experimental and computational studies on substituted 2,6-diarylphenols that demonstrate the essential contribution from through-space OH–π interactions and O^-–π interactions in the observed trends in proton affinities and acidities of 2,6-diarylphenols.

Noncovalent interactions play key roles in many genuinely important (bio)molecular processes.[1, 2] Although the nature and strength of many noncovalent interactions have been extensively studied, the link between molecular structure and properties remains a subject of ongoing molecular investigations.[3] Recent biomolecular studies revealed that the aromatic rings (i.e. π system) are involved in energetically favorable interactions between proteins and ligands *via* several types of polar–π interactions, including π–π interactions, cation–π interactions, anion–π interactions, SH–π interactions and OH–π interactions.[4, 5] Due to direct involvement of aromatic rings of amino acids of proteins in associations with small molecule inhibitors, an in-depth understanding of polar–π interactions importantly contributes to current rational drug design and development.[6]

Phenols represent an important class of aromatic molecules that display interesting physicochemical properties and biological activities.[7, 8] Physical-organic chemistry investigations on substituted phenols revealed that the acidity of phenol is significantly altered by electron-donating and electron-withdrawing groups at *ortho*-, *meta*-, or *para*-positions.[9-15] Notably, pK_a values of *para*-substituted phenols exhibit a linear dependence on the Hammett σ values. Collectively, chemical studies demonstrated that substituent effects on the acidity of phenols are primarily a result of through-bond mechanisms. Despite an important insight into the role of through-bond effects on the acidity of substituted phenols, the mechanistically distinct through-space effect has not been established to the same level of detail.[16-19]

Here we report the role of the through-space effect on the acidity of 2,6-diarylphenols (Figure 1). We conceived that the arrangement of two flanking aromatic rings around the central phenolic

ring in 2,6-diarylphenols enables detailed experimental and computational examinations of proposed through-space OH–π interactions at the unprecedented level of molecular detail. Physical-organic studies on the most related 2,6-diarylcarboxylic acids,[20] 2,6-diarylpyridines,[21] and 2,6-diarylanilines[22] revealed that the linear trends in acidities of such systems are a result of through-space effects (Figure 1). We hypothesized that the two neighboring flanking aromatic rings of 2,6-diarylphenols do not stabilize the protonated form of phenol *via* through-bond interactions, but rather *via* through-space OH–π interactions.

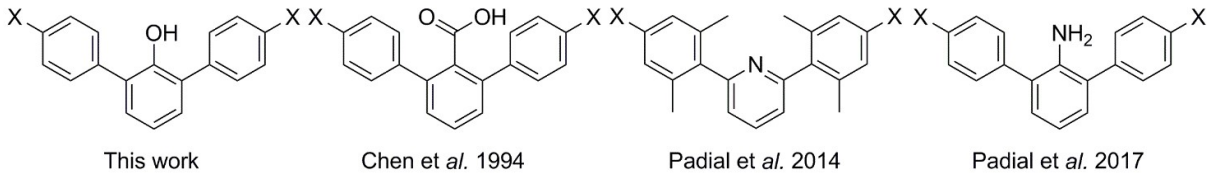

Figure 1. 2,6-Diaryl-substituted aromatic systems for physical-organic examinations of acidity.

2,6-Diarylphenols **1**–**6** were synthesized in three steps from 2,6-dibromophenol (Scheme 1). The phenolic OH of 2,6-dibromophenol was first protected by the acetyl group to afford 2,6-dibromophenol acetate, which then underwent the palladium-catalyzed Suzuki cross-coupling with arylboronic acids.[23] The basic hydrolysis of 2,6-diarylphenol acetates provided final 2,6-diarylphenols **1**–**6**.

Scheme 1. Synthesis of 2,6-Diarylphenols 1–6

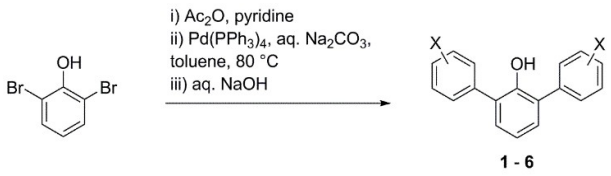

pK_a values of 2,6-diarylphenols **1**–**6** were measured by UV-vis spectroscopy in buffered aqueous solutions containing 20% DMSO (to make phenols **1**–**6** fully soluble) in the pH range of 8–13 (Table 1 and Figure S1).[24] A strong linear correlation ($R^2 > 0.99$) was observed for measured pK_a values of *para*-substituted 2,6-diarylphenols **1**–**5** against the Hammett σ_{para} values (Figure 2). As in the case of other 2,6-diaryl systems,[20-22] $2\sigma_{para}$ values were used in analysis, because 2,6-diarylphenols possess two flanking aromatic rings each having one *para*-substituent (Figure 2). The observed slope provided the ρ value of +1.1, which is essentially the same as the one found for 2,6-diarylanilines and 2,6-diarylpyridines.[21, 22] These results indicate that *para*-substituted donating groups (e.g. OMe, Me) make the neighboring flanking aromatic rings more electron-rich, thus leading to significant stabilization of 2,6-diarylphenols, as manifested by higher pK_a values (i.e. being weaker acids). In contrast, *para*-substituted withdrawing groups (e.g. F, CF_3) make the flanking aromatic

rings electron-deficient, thus resulting in lower pK_a values when compared to the 2,6-diphenylphenol reference. Collectively, these results support our hypothesis that the through-space OH–π interactions essentially contribute to stabilization of 2,6-diarylphenols. Notably, we also measured O-H stretching frequencies by IR spectroscopy; a linear trend (R^2 = 0.94) was observed for a series of *para*-substituted 2,6-diarylphenols (Table S1 and Figure S2). The lowest and highest O-H frequencies were measured for electron-donating OMe (**2**) and electron-withdrawing CF_3 (**5**), respectively, implying that favorable through-space OH–π interactions are present in 2,6-diarylphenols.

A further support for the presence of through-space OH–π interactions was obtained by comparisons of pK_a values of 2,6-diphenylphenols that bear *meta*-substituted F (**6**) and *para*-substituted F (**4**) (Table 1). *Meta*- and *para*-substituted F have significantly different values of the Hammett σ constant: 0.06 for *meta*-substituted F (**6**) and 0.34 for *para*-substituted F (**4**). Despite having substantially different σ values, **6** and **4** have comparable pK_a values of 11.24 and 11.29, respectively (Table 1). This observation importantly demonstrates that the through-bond resonance effect does not contribute to trends in pK_a values of 2,6-diarylphenols, because a full resonance stabilization (i.e. from the flanking rings to the central phenol ring) would only be possible for *para*-substituted F and not for *meta*-substituted F, thus leading to different pK_a values that we do not observe. As discussed below, the through-bond resonance effect is also excluded based on the nonplanar geometry of 2,6-diarylphenols. It is noteworthy that the through-bond inductive effect is also not contributing to observed pK_a trends of 2,6-diarylphenols, due to large distance of *para*-substituents (six bonds between the OH of phenol and the C_δ that has an attached substituent).

Table 1. pK_a Values for Phenols 1–6

compd	X	σ	pK_a[a]
1	H	0.00	11.38
2	*p*-OMe	–0.27	12.02
3	*p*-Me	–0.17	11.88
4	*p*-F	0.06	11.29
5	*p*-CF_3	0.54	10.29
6	*m*-F	0.34	11.24

[a] Determined in H_2O:DMSO = 4:1.

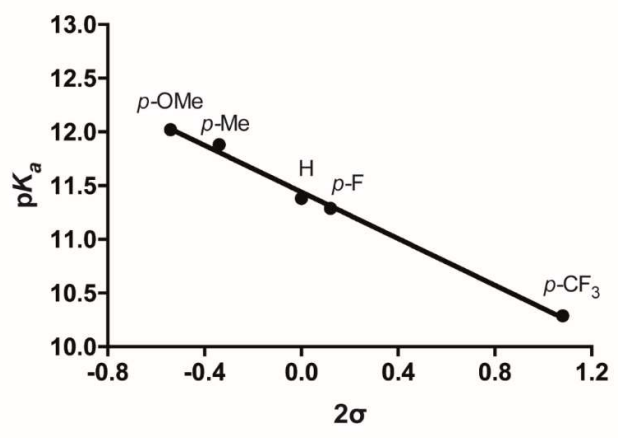

Figure 2. Correlation between pK_a values of phenols **1**–**5** and the Hammett sigma values (2σ).

We then attempted to solve a crystal structure of a representative 2,6-diarylphenol. Crystals of the phenol that bears the *para*-substituted F (**4**) were obtained from methanol at room temperature.[25] X-ray crystallographic data revealed that the structure has two independent diarylphenol molecules in the asymmetric unit and that the three aromatic rings in **4** are not coplanar. Dihedral angles between the middle phenol ring and both flanking aromatic rings were observed to be in the range of 31–69° (Figures 3 and S3 and Table S2). Aromatic rings appear to be both in ‘‘parallel’’ or ‘‘eclipsed’’ conformation (i.e. both flanking aromatic rings are pointed in the same direction relative to the central phenol ring) and ‘‘antiparallel’’ or ‘‘staggered’’ conformation (i.e. both flanking aromatic rings are pointed in the opposite direction relative to the central phenol ring) (Figure 3). Both arrangements, however, enable a formation of strong hydrogen bond between the phenolic OH and the electron-rich aromatic system of the adjacent aromatic rings. The shortest distances between the hydrogen atom of OH and the carbon atom of the flanking rings were measured to be: OH-C_α 2.4 Å, OH-C_β 2.2 Å, OH-C_γ 3.4 Å, and OH-C_δ 4.2 Å. In dimer, the shortest distance between hydrogen atoms in OH–HO is 2.6 Å.

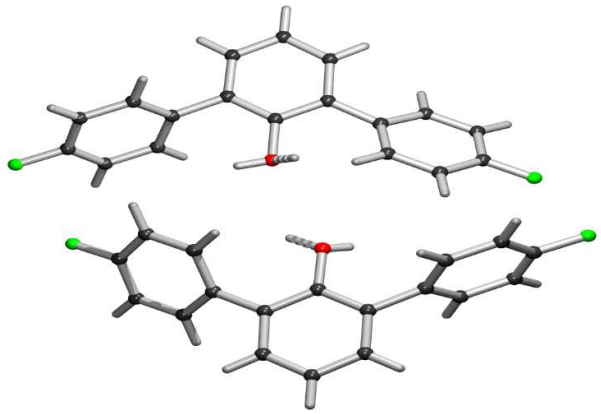

Figure 3. View on the crystal structure of **4**.

Having shown that quantum chemical analyses on related 2,6-diarylanilines and 2,6-diarylpyridines provided an important insight into energetics and geometry,[21, 22] we used the same computational approach to examine through-space polar–π interactions in 2,6-diarylphenols (Figure 4). In particular, we were interested in: 1) dependence of energy (enthalpy) change for ArOH → ArO^- + H^+ on the substituent X; and 2) for X = H, rotational barrier for internal rotation around C-C bond of XPh—ArOH (rotation of one single XPh- substituent, i.e. the lowest energy of X = H is computed and then we calculate the rotational barrier around C-C for one ring while keeping the other at the lowest energy conformation). The computational analyses were done using the ADF program at the BLYP-D3BJ/TZ2P level of DFT in aqueous solvation simulated using COSMO (Tables S3–S11).[26]

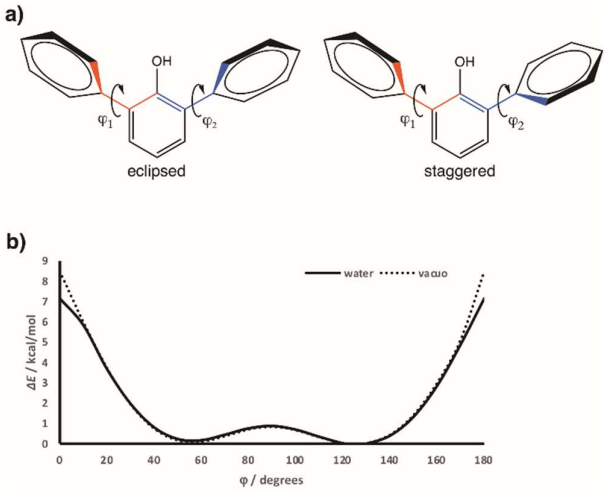

Figure 4. a) Eclipsed and staggered conformations for 2,6-diarylphenol. Dihedral φ_1 corresponds to HOC-C_2-C_α-C_β and φ_2 to HOC-C_6-C_α-C_β angles. b) Dependence of the relative energy ΔE (in kcal mol^{-1}) of 2,6-diphenylphenol (**1**) with the rotation of the HOC-C_2-C_α-C_β dihedral angle (φ, in degrees) in water and in gas phase.

The panel of 2,6-diarylphenols **1**–**6** was optimized, and two conformations appear to be nearly isoenergetic (Table 2 and Figure 4a) with respect to the dihedral angles with the two aryl rings: parallel or eclipsed vs. antiparallel or staggered. Similar energetics of eclipsed and staggered orientations are in line with observed conformations in the crystal state (see above). Both in water and in the gas phase, the eclipsed conformation is slightly more stable by a maximum of 0.27 kcal mol^{-1}. The calculated HOC-C_2-C_α-C_β and HOC-C_6-C_α-C_β dihedral angles for the eclipsed and the staggered conformation (Table S12) are in line with those obtained from structural characterization of **4** (see above).

The almost isoenergetic eclipsed and staggered conformations for this set of systems has been also confirmed by the calculation of the rotational barrier for 2,6-diarylphenol (**1**, X = H) in the range 0–180º (Figure 4b). Note that only one HOC-C_2-C_α-C_β dihedral angle was varied, whereas the other dihedral angle was kept at 50.2º (water) or 47.8º (gas phase). The most unstable conformers are those close to either 0 or 180º, whereas those in the range 40–140º differ by less than 1 kcal mol^{-1}.

Table 2. Energies of Eclipsed and Staggered Conformations and Proton Affinities for both Conformations in Water and in the Gas Phase in the Series of 2,6-Diarylphenols 1–6 (in kcal mol^{-1})

		water			*vacuo*		
compd	**X**	$\Delta\Delta E_{\text{ecli-stag}}$	$\Delta E^{\text{PA}}_{\text{ecli}}$	$\Delta E^{\text{PA}}_{\text{stag}}$	$\Delta\Delta E_{\text{stag-ecli}}$	$\Delta E^{\text{PA}}_{\text{ecli}}$	$\Delta E^{\text{PA}}_{\text{stag}}$
1	H	–0.18	174.9	174.7	–0.10	342.0	342.0
2	*p*-OMe	–0.27	176.5	176.1	–0.16	344.3	344.5
3	*p*-Me	–0.21	176.0	175.7	–0.13	343.6	343.6
4	*p*-F	–0.18	174.3	174.1	–0.11	337.1	337.1
5	*p*-CF_3	–0.18	172.2	172.1	–0.08	328.0	328.0
6	*m*-F	–0.15	173.1	172.9	–0.09	335.8	335.9

Next, we have calculated the proton affinities of all the substituted 2,6-diarylphenols (ΔE^{PA}, Table 2). It can be observed that both conformations present almost the same ΔE^{PA} values. The ΔE^{PA} for the eclipsed conformation has been plotted against twice the Hammett constant (2σ), both in water and in the gas phase (Figure 5 and S4). Good correlations were observed, both in water (Figure 5) and in vacuo (Figure S4); in water the slope is –2.67 ($R^2 = 0.99$), whereas in the gas phase the slope is –10.6 ($R^2 = 0.95$). The observed larger slope in the gas phase than in water indicates that the proton affinities in the gas phase are significantly larger than those in water, which we attribute to much stronger solvation of the proton than of the protonated phenol (and the phenol). In addition, an

observation that *meta*- and *para*-substituted F have similar proton affinities provided additional support for the presence of through-space interactions in 2,6-diarylphenols (Table 2).

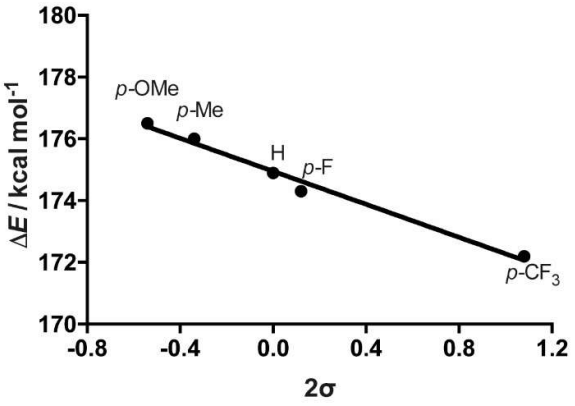

Figure 5. Correlation between proton affinities ΔE in water and the Hammett sigma values (2σ) of phenols **1**–**5** in an eclipsed conformation.

We then investigated the foundation of the *para*-substituent effect on the proton affinities of 2,6-diarylphenols **2** and **5** with the largest PA (OMe, 176.5 kcal mol^{-1}) and the lowest PA (CF_3, 172.2 kcal mol^{-1}). We have analyzed the interaction between one substituted benzene ring (Aryl) and either H_2O or OH^- (Table 3 and Figure S5). We previously performed a similar procedure to study the origin of through-space cation–π interactions in *para*-substituted 2,6-diarylanilines.[22] The interaction ΔE_{int} in the case of *p*CF_3 (–1.1 kcal mol^{-1}) is less stabilizing than that of *p*OMe (–1.3 kcal mol^{-1}; Table 3), in line with measured (*vide supra*) and computed (*vide infra*) O–H stretch frequencies. Note however that these OH–π interactions are relatively weak and, thus, contribute little to the difference in PA values. Thus, the difference in the PA must be found in the deprotonated systems, i.e. with the hydroxyl fragment. And indeed, ΔE_{int} in the case of the *p*CF_3^- (–20.9 kcal mol^{-1}) is clearly more stabilizing than in the case of *p*OMe^- (–11.4 kcal mol^{-1}). The EDA decomposition of these latter ΔE_{int} into electrostatic, Pauli, and orbital interaction terms provided evidence that such difference is due to ΔV_{elstat}, which is reduced from –8.7 to –0.7 kcal mol^{-1} as we go from *p*CF_3^- to *p*OMe^-. On the other hand, both substituents present similar ΔE_{Pauli} and ΔE_{oi} magnitudes (Table 3). Note that the interaction with OH^- is significantly more attractive than with water, despite Pauli repulsion is quite similar to the previous case. To investigate the much smaller contribution of ΔV_{elstat} in *p*OMe^- than in *p*CF_3^-, the Voronoi Deformation Density (VDD) charges were calculated (Figure 6 and Table S13) for both separate fragments for either *p*CF_3^- and *p*OMe^- systems. More negatively charged carbon atoms were found in the latter case, reflecting the electron-pushing character of OMe as compared to the electron-pulling character of CF_3. This statement is also supported by the isosurface of the molecular electrostatic potential of both *p*OMe to *p*CF_3 depicted in Figure 6, in which the π system of *p*OMe

appears more negative (more red). Thus, the more positively charged *p*CF_3-substituted aryl rings interact more favorably with the hydroxyl anion, as revealed by our EDA analysis (Table 3). This also leads to a somewhat shorter HO^-–Aryl distance in *p*CF_3 (2.896 Å) than in *p*OMe (2.903 Å, see Table S13).

Table 3. Through-space interaction analyses (in kcal mol^{-1}) in simplified models of *para*-substituted 2,6-diarylphenols and their conjugate bases.[a]

	System	Interaction	ΔE_{int}	ΔE_{Pauli}	ΔV_{elstat}	ΔE_{oi}	ΔE_{disp}
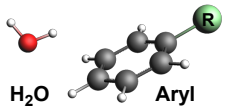	*p*CF_3	$H_2O\cdots$Aryl(CF_3)	–1.1	8.8	–4.8	–2.9	–2.2
	*p*OMe	$H_2O\cdots$Aryl(OMe)	–1.3	9.5	–5.3	–3.2	–2.3
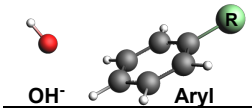	*p*CF_3^-	$OH^-\cdots$Aryl(CF_3)	–20.9	7.6	–8.7	–18.4	–1.4
	pOMe^-	$OH^-\cdots$Aryl(OMe)	–11.4	7.8	–0.7	–17.2	–1.4

[a] See Figure S5. Calculated at ZORA-BLYP-D3BJ/TZ2P level of theory. As the values of eclipsed and staggered conformations are almost the same, only the former ones are enclosed.

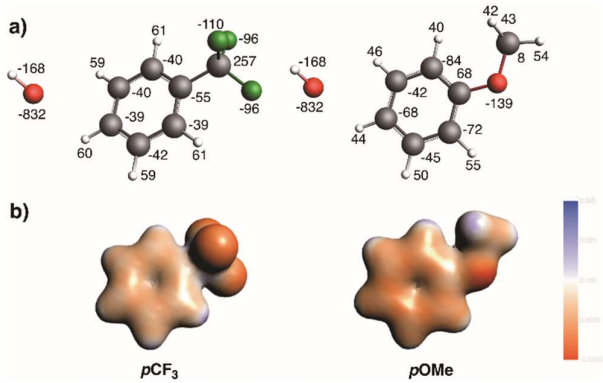

Figure 6. a) VDD charges (in milli-electrons) for fragments in model systems used in through-space interaction analysis for *p*CF_3^- and *p*OMe^- (see Table 3), and b) molecular electrostatic potential isosurfaces for *p*CF_3 and *p*OMe, calculated at ZORA-BLYP-D3BJ/TZ2P level.

Finally, we also calculated O-H stretching frequency shifts of the series of 2,6-diarylphenols **1–6** in water and in the gas phase (Table S14 and Figures S6–S7). In line with the experimentally observed trend, we found that electron-donating groups lead to frequency lowering, whereas electron-withdrawing groups show frequency increasing, for both eclipsed and staggered conformations (R^2 = 0.88–0.96) (Figures S6–S7). These results demonstrate that electron-rich flanking aromatic rings form stronger OH–π interactions with the OH group of the central phenol.

In conclusion, we have demonstrated that 2,6-diarylphenols are stabilized by a combination of intramolecular OH–π interactions and, interestingly, O^-–π interactions, as manifested by linear correlations in pK_a values and proton affinities for 2,6-diarylphenols that bear *para*-substituents at the two neighboring aromatic rings. Unlike many substituted phenols whose acidity is strongly affected by the through-bond effect, the acidity of 2,6-diarylphenols is influenced by the mechanistically distinct through-space effect. Along with physical-organic chemistry examinations of related molecular systems,[20-22, 27, 28] the work further highlights that the 2,6-diaryl substituted aromatic scaffolds are good models for studying the role of the through-space effect between polar functional groups and aromatic rings.

EXPERIMENTAL SECTION

Synthesis of 2,6-diarylphenols.

To a mixture of 2,6-dibromophenol acetate[23] (0.5 mmol) and $Pd(PPh_3)_4$ (0.1 mmol) in toluene (4 mL) were added a solution of the arylboronic acid (1 mmol) in THF (5 mL) and an aqueous solution of Na_2CO_3 (2 M, 2 mL). After refluxing at 80 °C for 18 hours, the reaction mixture was poured into 20 mL of water and extracted with 20 mL of diethyl ether. The combined organic layers were dried with $MgSO_4$, filtered and evaporated *in vacuo* to obtain acetylated 2,6-diarylphenols that were deacetylated using an aqueous solution of NaOH (2M, 5 ml) and then acidified with HCl (2M, 6 ml) and extracted with ethyl acetate (2 × 20 ml). The products were purified by column chromatography using heptane with an increasing gradient (0–50%) of ethyl acetate to afford 2,6-diarylphenols **1**–**6**.

2,6-Diphenylphenol (1): White solid (67 mg, 55% yield); mp 102–103 °C; ^{1}H NMR (400 MHz, $CDCl_3$) δ 5.40 (1H, s), 7.06 (1H, t, J = 7.0 Hz), 7.25–7.30 (2H, m), 7.38–7.40 (2H, m), 7.45–7.50 (4H, m), 7.54–7.58 (4H, m); ^{13}C{^{1}H} NMR (101 MHz, $CDCl_3$) δ 120.7, 127.7, 128.8, 128.9, 129.4, 130.0, 137.6, 149.3; HRMS (EI-TOF) [M^+] *m/z*: calcd for $C_{18}H_{14}O$ 246.1045; found; 246.1045.

2,6-Di(4-methoxy)phenylphenol (2): Red solid (20 mg, 13% yield); mp 102–103 °C; ^{1}H NMR (400 MHz, $CDCl_3$) δ 3.84 (6H, s), 5.36 (1H, s) 6.95 (2H, d, J = 9.0 Hz), 7.00–7.02 (2H, m), 7.22 (1H, d, J = 8.0 Hz), 7.34 (2H, s), 7.38–7.40 (2H, d), 7.49 (2H, d, J = 9.0 Hz); ^{13}C{^{1}H} NMR (101 MHz, $CDCl_3$) δ 55.3, 113.7, 114.3, 126.4, 129.4, 129.5, 129.7, 130.1, 130.5, 130.7; HRMS (EI-TOF) [M^+] *m/z*: calcd for $C_{20}H_{18}O_3$ 306.1256; found; 306.1271.

2,6-Di(4-methyl)phenylphenol (3): White solid (30 mg, 22% yield); mp 94–95 °C; ^{1}H NMR (400 MHz, $CDCl_3$) δ 2.38 (6 H, s), 7.21 (4H, d, J = 6.5 Hz), 7.20–7.24 (1H, m), 7.34 (4H, d, J = 7.0 Hz), 7.35 (2 H, s), 7.43–7.45 (1 H, m); ^{13}C{^{1}H} NMR (101 MHz, $CDCl_3$) δ 21.2, 128.8, 129.0, 129.9,

129.6, 129.9, 135.0, 135.7, 137.2; HRMS (EI-TOF) [M^+] *m/z*: calcd for $C_{20}H_{18}O$ 274.1358; found; 274.1368.

2,6-Di(4-fluoro)phenylphenol (4): White solid (128 mg, 91% yield); mp 66–67 °C; ^{1}H NMR (400 MHz, $CDCl_3$) δ 5.23 (1H, s), 7.05 (1H, t, *J* = 7.0 Hz), 7.11–7.19 (4H, m), 7.23–7.26 (2H, m), 7.48–7.55 (4H, m); $^{13}C\{^1H\}$ NMR (101 MHz, $CDCl_3$) δ 115.7, 120.8, 122.9, 130.1, 131.0, 133.3, 149.3, 161.2, 163.6; HRMS (EI-TOF) [M^+] *m/z*: calcd for $C_{18}H_{12}F_2O$ 282.0856; found; 282.0851.

2,6-Di(4-trifluoromethyl)phenylphenol (5): Orange solid (120 mg, 63% yield); mp 97–98 °C; ^{1}H NMR (400 MHz, $CDCl_3$) δ 5.23 (1H, s), 7.12 (1H, dd, *J* = 7.5 Hz, 8.0 Hz), 7.31 (1 H, d, *J* = 7.5 Hz), 7.42–7.45 (1H, m), 7.57 (2H, d, *J* = 7.5 Hz), 7.67–7.70 (3H, m), 7.73–7.77 (2H, m); $^{13}C\{^1H\}$ NMR (101 MHz, $CDCl_3$) δ 121.3, 125.3, 125.9, 126.9, 127.6, 129.4, 129.8, 130.7, 134.9; HRMS (EI-TOF) [M^+] *m/z*: calcd for $C_{20}H_{12}F_6O$ 382.0792; found; 382.0792.

2,6-Di(3-fluoro)phenylphenol (6): White solid (80 mg, 57% yield); mp 86–87 °C; ^{1}H NMR (400 MHz, $CDCl_3$) δ 5.36 (1H, s), 7.03–7.09 (2H, m), 7.15–7.20 (2H, m), 7.21–7.24 (2H, m), 7.35–7.45 (5H, m); $^{13}C\{^1H\}$ NMR (101 MHz, $CDCl_3$) δ 113.41, 113.62, 114.87, 115.09, 123.71, 123.72, 125.67, 128.78, 128.86, 129.34; HRMS (EI-TOF) [M^+] *m/z*: calcd for $C_{18}H_{12}F_2O$ 282.0856; found; 282.0864.

Quantum chemical analyses.

All calculations were carried out with the Amsterdam Density Functional (ADF) program using dispersion-corrected density functional theory at the BLYP-D3BJ/TZ2P level of theory.[26, 29] The effect of solvation in water was simulated by means of the Conductor like Screening Model (COSMO) of solvation as implemented in ADF. The approach has been benchmarked against highly correlated post-Hartree-Fock methods and experimental data and was found to work reliably.[21, 30, 31] The bonding mechanism of water (taken from phenol) or hydroxyl (taken from unprotonated phenol) with the two substituted benzene rings (taken from aryl rings) was analyzed within the framework of quantitative Kohn-Sham molecular orbital theory[32] in combination with a quantitative energy decomposition analysis (EDA)[32] in the gas phase. The electronic bond energy ΔE can be decomposed into the strain energy ΔE_{strain} associated with deforming the fragments from their equilibrium structure to the geometry they adopt in modified aniline, plus the interaction energy ΔE_{int} between these deformed fragments. The latter is further decomposed into the classical electrostatic attraction ΔV_{elstat}, Pauli repulsion ΔE_{Pauli} between occupied orbitals, stabilizing orbital interactions ΔE_{oi}, and dispersion $\Delta E_{disp.}$ Atomic charges were computed with the Voronoi deformation density (VDD) method.[33]

ASSOCIATED CONTENT

Supporting Information

The Supporting Information is available free of charge on the ACS Publications website.

NMR spectra, pK_a measurements, IR data, X-ray crystallography data, computational studies.

Crystallographic data for **4**.

AUTHOR INFORMATION

Corresponding Authors

*E-mail: mecinovic@sdu.dk

*E-mail: f.m.bickelhaupt@vu.nl

ORCID

Jordi Poater: 0000-0002-0814-5074

Roel Hammink: 0000-0001-8721-5271

F. Matthias Bickelhaupt: 0000-0003-4655-7747

Jasmin Mecinović: 0000-0002-5559-3822

Author Contributions

⊥ These authors contributed equally to this work.

Notes

The authors declare no competing financial interest.

ACKOWLEDGMENTS

We thank the Netherlands Organization for Scientific Research (NWO) for financial support. J.P. thanks the Spanish MINECO (CTQ2016-77558-R and MDM-2017-0767) and the Generalitat de Catalunya (2017SGR348).

REFERENCES

1. Cockroft, S. L.; Hunter, C. A., Chemical double-mutant cycles: dissecting non-covalent interactions. *Chem. Soc. Rev.* **2007,** *36*, 172-188.
2. Karshikoff, A., *Non-Covalent Interactions in Proteins*. Imperial College Press: London, 2006.
3. Müller-Dethlefs, K.; Hobza, P., Noncovalent Interactions: A Challenge for Experiment and Theory. *Chem. Rev.* **2000,** *100*, 143-168.
4. Meyer, E. A.; Castellano, R. K.; Diederich, F., Interactions with Aromatic Rings in Chemical and Biological Recognition. *Angew. Chem. Int. Ed.* **2003,** *42*, 1210-1250.
5. Salonen, L. M.; Ellermann, M.; Diederich, F., Aromatic Rings in Chemical and Biological Recognition: Energetics and Structures. *Angew. Chem. Int. Ed.* **2011,** *50*, 4808-4842.
6. Shanshan, L.; Yuan, X.; Qiancheng, S.; Xian, L.; Jing, L.; Yadong, C.; Tao, L.; Cheng, L.; Xiaomin, L.; Mingyue, Z.; Hualiang, J., Non-Covalent Interactions with Aromatic Rings: Current Understanding and Implications for Rational Drug Design. *Curr. Pharm. Des.* **2013,** *19*, 6522-6533.
7. Puupponen-Pimiä, R.; Nohynek, L.; Meier, C.; Kähkönen, M.; Heinonen, M.; Hopia, A.; Oksman-Caldentey, K.-M., Antimicrobial properties of phenolic compounds from berries. *J. Appl. Microbiol.* **2001,** *90*, 494-507.
8. Rappaport, Z., *The Chemistry of Phenols*. John Wiley & Sons, Ltd2003.
9. Biggs, A. I.; Robinson, R. A., 69. The ionisation constants of some substituted anilines and phenols: a test of the Hammett relation. *J. Chem. Soc.* **1961**, 388-393.
10. Fickling, M. M.; Fischer, A.; Mann, B. R.; Packer, J.; Vaughan, J., Hammett Substituent Constants for Electron-withdrawing Substituents: Dissociation of Phenols, Anilinium Ions and Dimethylanilinium Ions. *J. Am. Chem. Soc.* **1959,** *81*, 4226-4230.
11. Liptak, M. D.; Gross, K. C.; Seybold, P. G.; Feldgus, S.; Shields, G. C., Absolute pKa Determinations for Substituted Phenols. *J. Am. Chem. Soc.* **2002,** *124*, 6421-6427.
12. Pratt, D. A.; DiLabio, G. A.; Mulder, P.; Ingold, K. U., Bond Strengths of Toluenes, Anilines, and Phenols: To Hammett or Not. *Acc. Chem. Res.* **2004,** *37*, 334-340.
13. Silva, P. J., Inductive and Resonance Effects on the Acidities of Phenol, Enols, and Carbonyl α-Hydrogens. *J. Org. Chem.* **2009,** *74*, 914-916.
14. Svobodová Vařeková, R.; Geidl, S.; Ionescu, C.-M.; Skřehota, O.; Kudera, M.; Sehnal, D.; Bouchal, T.; Abagyan, R.; Huber, H. J.; Koča, J., Predicting pKa Values of Substituted Phenols from Atomic Charges: Comparison of Different Quantum Mechanical Methods and Charge Distribution Schemes. *J. Chem. Inf. Model.* **2011,** *51*, 1795-1806.
15. Gross, K. C.; Seybold, P. G., Substituent effects on the physical properties and pKa of phenol. *Int. J. Quantum Chem.* **2001,** *85*, 569-579.
16. Nakatsu, K.; Yoshioka, H.; Kunimoto, K.; Kinugasa, T.; Ueji, S., 2,6-Diphenylphenol: a structure containing an intramolecular O-H...[pi] hydrogen bond. *Acta Cryst. B* **1978,** *34*, 2357-2359.
17. Nikolova, V.; Ilieva, S.; Galabov, B.; Schaefer, H. F., Experimental Measurement and Theory of Substituent Effects in π-Hydrogen Bonding: Complexes of Substituted Phenols with Benzene. *J. Org. Chem.* **2014,** *79*, 6823-6831.
18. Vojta, D.; Vazdar, M., The study of hydrogen bonding and π···π interactions in phenol···ethynylbenzene complex by IR spectroscopy. *Spectrochim. Acta Part A: Mol. Biomol. Spectrosc.* **2014,** *132*, 6-14.

19. Wheeler, S. E.; Houk, K. N., Through-Space Effects of Substituents Dominate Molecular Electrostatic Potentials of Substituted Arenes. *J. Chem. Theory Comput.* **2009,** *5*, 2301-2312.
20. Chen, C.-T.; Siegel, J. S., Through-Space Polar-.pi. Effects on the Acidity and Hydrogen-Bonding Capacity of Carboxylic Acids. *J. Am. Chem. Soc.* **1994,** *116*, 5959-5960.
21. Simó Padial, J.; de Gelder, R.; Fonseca Guerra, C.; Bickelhaupt, F. M.; Mecinović, J., Stabilisation of 2,6-Diarylpyridinium Cation by Through-Space Polar–π Interactions. *Chem. Eur. J.* **2014,** *20*, 6268-6271.
22. Simó Padial, J.; Poater, J.; Nguyen, D. T.; Tinnemans, P.; Bickelhaupt, F. M.; Mecinović, J., Stabilization of 2,6-Diarylanilinum Cation by Through-Space Cation−π Interactions. *J. Org. Chem.* **2017,** *82*, 9418-9424.
23. Kimura, M.; Nomoto, H.; Masaki, N.; Mori, S., Dye Molecules for Simple Co-Sensitization Process: Fabrication of Mixed-Dye-Sensitized Solar Cells. *Angew. Chem. Int. Ed.* **2012,** *51*, 4371-4374.
24. Martínez, C. H. R.; Dardonville, C., Rapid Determination of Ionization Constants (pKa) by UV Spectroscopy Using 96-Well Microtiter Plates. *ACS Med. Chem. Lett.* **2013,** *4*, 142-145.
25. *CCDC 1882991 contains the supplementary crystallographic data for this paper.*
26. te Velde, G.; Bickelhaupt, F. M.; Baerends, E. J.; Fonseca Guerra, C.; van Gisbergen, S. J. A.; Snijders, J. G.; Ziegler, T., Chemistry with ADF. *J. Comput. Chem.* **2001,** *22*, 931-967.
27. Annunziata, R.; Benaglia, M.; Cozzi, F.; Mazzanti, A., The Intramolecular Edge-to-Face Interactions of an Aryl C-H Bond and of a Pyridine Nitrogen Lone-Pair with Aromatic and Fluoroaromatic Systems in Some [3,3]Metaparacyclophanes: A Combined Computational and NMR Study. *Chem. Eur. J.* **2009,** *15*, 4373-4381.
28. Duttwyler, S.; Do, Q.-Q.; Linden, A.; Baldridge, K. K.; Siegel, J. S., Synthesis of 2,6-Diarylphenyldimethylsilyl Cations: Polar-π Distribution of Cation Character. *Angew. Chem. Int. Ed.* **2008,** *47*, 1719-1722.
29. Becke, A. D., Density-functional exchange-energy approximation with correct asymptotic behavior. *Phys. Rev. A* **1988,** *38*, 3098-3100.
30. Fonseca Guerra, C.; van der Wijst, T.; Poater, J.; Swart, M.; Bickelhaupt, F. M., Adenine versus guanine quartets in aqueous solution: dispersion-corrected DFT study on the differences in π-stacking and hydrogen-bonding behavior. *Theor. Chem. Acc.* **2010,** *125*, 245-252.
31. van der Wijst, T.; Fonseca Guerra, C.; Swart, M.; Bickelhaupt, F. M.; Lippert, B., A Ditopic Ion-Pair Receptor Based on Stacked Nucleobase Quartets. *Angew. Chem. Int. Ed.* **2009,** *48*, 3285-3287.
32. Wolters, L. P.; Bickelhaupt, F. M., The activation strain model and molecular orbital theory. *WIRES Comput. Mol. Sci.* **2015,** *5*, 324-343.
33. Fonseca Guerra, C.; Handgraaf, J.-W.; Baerends, E. J.; Bickelhaupt, F. M., Voronoi deformation density (VDD) charges: Assessment of the Mulliken, Bader, Hirshfeld, Weinhold, and VDD methods for charge analysis. *J. Comput. Chem.* **2004,** *25*, 189-210.